Hindawi
Geofluids
Volume 2022, Article ID 3415409, 20 pages
https://doi.org/10.1155/2022/3415409

Research Article

Productivity Prediction and Simulation Verification of Fishbone Multilateral Wells

Wen Jing,[1] Liu Xiao,[2] Hu Haixia,[3] and Luo Wei[4,5,6,7]

[1]Institute of Mud Logging Technology and Engineering, Yangtze University, Jingzhou 434023, China
[2]Sichuan Shale Gas Exploration and Development Limited Liability Company, Chengdu 640000, China
[3]College of Technology & Engineering, Yangtze University, Jingzhou 434000, China
[4]Petroleum Engineering Institute of Yangtze University, Wuhan, Hubei 430100, China
[5]Gas Lift Innovation Center, Laboratory of Multiphase Pipe Flow, Yangtze University, CNPC, Wuhan 430100, China
[6]State Key Laboratory of Shale Oil and Gas Enrichment Mechanisms and Effective Develpment, Beijing 100083, China
[7]Sinopec Key Laboratory of Shale Oil/Gas Exploration and Production Technology, Beijing 100083, China

Correspondence should be addressed to Hu Haixia; zijiatp@163.com

Received 26 March 2022; Revised 12 August 2022; Accepted 22 August 2022; Published 25 September 2022

Academic Editor: Zhiyuan Wang

As fishbone multilateral wells are increasingly used in the development of oil and gas fields, the need for the optimal design of multilateral well parameters has become increasingly urgent. Although the establishment of multilateral well productivity models has taken a step forward due to recently contributed research results, there are still few studies on model verification; that is, these models lack verification, and their reliability is uncertain, which increases the difficulty of their promotion and application in practice. Therefore, based on a more comprehensive horizontal well productivity prediction model, a fishbone multilateral well productivity prediction model was established in this work. Taking an oil field in the Middle East as an example, multilateral well productivity prediction and parameters sensitivity analysis were carried out, and the results were compared with the simulation results determined by using CMG digital simulation software. The established model was verified in terms of branch length, branch angle, and branch output contribution. The conclusions reached by these two methods were consistent, which verified that the established model was reliable.

1. Introduction

Multilateral wells have been increasingly used by oil and gas companies due to their advantages [1] in increasing the contact area between wellbores and reservoirs, delaying production decline and improving oil and gas recovery. Fishbone multilateral wells are widely used and are one of the important types of multilateral wells. In the process of development with fishbone wells, the design optimization of the branch parameters of the fishbone wells is inevitable. How to maximize the development advantages of fishbone wells in the development process is the key research and concern of the majority of researcher in the oil and gas industry.

With the continuous development of production and scientific research, many branched well productivity prediction models and parameters optimization theories have emerged at home and abroad. Basquet et al. [2] established a semianalytical model for productivity evaluation of inclined wells in multilayer reservoirs by using the microelement method to divide fishbone multilateral wells into several small sections and couple seepage and wellbore flow. Retnanto et al. [3] used the analytical method and variable mass flow semianalytical method to establish a model but only considered several symmetric branched wells with fixed angles, which had limitations in application. Huang et al. [4] established a well test interpretation model of variable mass flow in fishbone multilateral horizontal wells by using Green's function and the Newman product method. Li et al. [5, 6] simplified the seepage problem by dividing the seepage field. An approximate formula for the steady-state productivity of fishbone wells was obtained by conformal transformation and equivalent seepage resistance theory, which was verified by hydropower simulation tests, but the variable mass flow in the wellbore was ignored. Based on the study of the horizontal well productivity prediction model, Liu et al. [7] deduced a fishbone well coupling model and showed that this development method is more suitable for thin-bottom-water reservoirs. Duan et al. [8] established a mathematical model of the pressure distribution in branched horizontal wells based on the pressure distribution model along horizontal wells. Yongsheng et al. [9, 10] analyzed the influence of design parameters of fishbone multilateral wells on productivity by using an analytical model and proposed a design parameter optimization theory. Le et al. [11] used the characteristics of a constant pressure supply at the lower boundary of a reservoir with bottom water, established relevant models with the concept of microelements, and used reservoir subdivision instead of wellbore subdivision to reduce the calculation amount.

Most of the existing studies have established only a productivity prediction model for fishbone wells; these models not only have some disadvantages, such as ignoring the wellbore variable mass flow pressure drop, branch interference, branch angle, and pressure superposition of the whole drainage area and the calculation defects of the model itself, but also lack comparative verification. In view of this, in this paper, based on a comprehensive horizontal well productivity prediction model [12], a coupling model considering the mutual interference of formation seepage between the branches of fishbone wells and the interaction of wellbore junctions is deduced and established, and a solution method is obtained. Then, the calculated results are compared with the results from numerical simulation software CMG for an example.

2. Productivity Prediction Method of Fishbone Multilateral Wells

Luo et al. have carried out many studies on horizontal well productivity prediction. In reference [12], a productivity prediction model that can consider the real wellbore trajectory is proposed for the influence of the real wellbore trajectory. In reference [13], a variable mass flow calculation model considering the real flow is proposed for the horizontal annulus effect. In reference [14], a prediction model for the transient productivity of horizontal wells is proposed in view of the influence of reservoir production time. In view of this, based on the basic model of Luo et al. [12], the research on the productivity prediction model of fishbone lateral wells was carried out. First, the relationship equation between pressure and production of each segment of the horizontal wellbore with nonuniform flow is deduced, and then the relationship equation between each segment and production of multibranch wells in fishbone well is established.

2.1. Calculation of Three Dimensional Space Potential of Uniform Inflow Horizontal Section (Real Well Trajectory). Assuming a point M in space, according to the seepage theory, with M point as the center, Q as the output, and the seepage velocity of the spherical surface with any R radius is

$$v = \frac{q}{4\pi r^2}. \tag{1}$$

At the same time, according to the definition of potential and Darcy's law

$$v = \frac{d\phi}{dr}. \tag{2}$$

The above two formulas are equal

$$\frac{q}{4\pi r^2} = \frac{d\phi}{dr}. \tag{3}$$

The expression of the space potential obtained by separating two equations and integrating them is

$$\phi = -\frac{q}{4\pi r} + C. \tag{4}$$

In the unbounded three-dimensional stratum, a horizontal well measuring length L (as shown in Figure 1) is in production. The coordinates of the heel and toe are (x_1, y_1, z_1) and (x_2, y_2, z_2). Assuming that steady-state seepage of single-phase crude oil in the formation, horizontal well is a line of uniform inflow.

The horizontal well is divided into m segments by length. It can be seen that when m is large enough, each segment can be approximated as a straight segment. The length of each segment is L/m, the starting coordinate of each segment is (x_{si}, y_{si}, z_{si}), and the coordinates of the end point are (x_{ei}, y_{ei}, z_{ei}), in which $i = 1, 2, 3, \cdots m$.

Take a point on one of the segments, the coordinates are (x, y, z), and as the end point, the distance from the beginning of the segment is

$$s = \sqrt{(x - x_{si})^2 + (y - y_{si})^2 + (z - z_{si})^2}. \tag{5}$$

By taking the full differential on both sides of the equation, the microelement ds is satisfied:

$$ds = \frac{1}{s}\left[(x - x_{si})dx + (y - y_{si})dy + (z - z_{si})dz\right]. \tag{6}$$

For the microelement ds, the flow of the microelement is $dq = (q/L)ds$, the potential generated in the space (X, Y, Z) is

$$d\phi = -\frac{dq}{4\pi r}, \tag{7}$$

$$d\phi = -\frac{q}{4\pi r L}ds, \tag{8}$$

$$d\phi = -\frac{q}{4\pi r L}\frac{1}{s}\left[(x - x_{si})dx + (y - y_{si})dy + (z - z_{si})dz\right]. \tag{9}$$

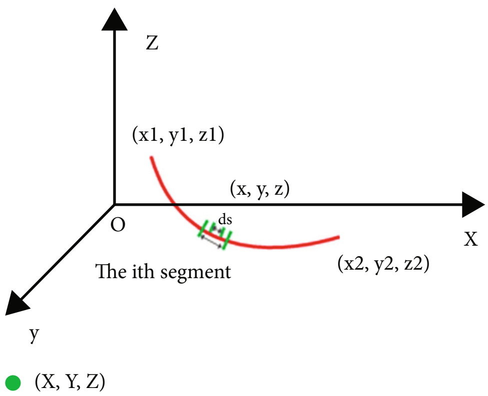

FIGURE 1: Schematic diagram of horizontal wells in unbounded strata.

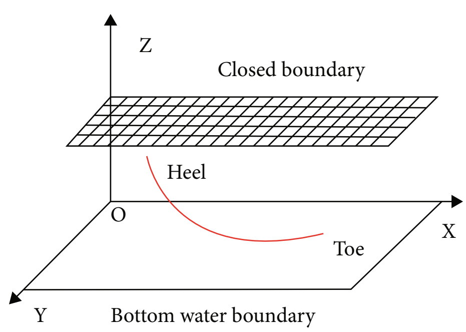

FIGURE 2: Schematic diagram of horizontal wells in top closed bottom water flooding reservoir.

Assuming, $f(x, y, z)$, $g(x, y, z)$, and $h(x, y, z)$, respectively, are

$$f(x, y, z) = -\frac{q}{4\pi rL}\frac{1}{s}(x - x_{si}), \quad (10)$$

$$g(x, y, z) = -\frac{q}{4\pi rL}\frac{1}{s}(y - y_{si}), \quad (11)$$

$$h(x, y, z) = -\frac{q}{4\pi rL}\frac{1}{s}(z - z_{si}). \quad (12)$$

Then, the spatial region belongs to the three-dimensional single-connected open region G, and $f(x, y, z)$, $g(x, y, z)$, and $h(x, y, z)$ have a first-order continuous partial derivative in G (for the microelement, r is a constant), which satisfies

$$\frac{\partial f}{\partial y} = \frac{\partial g}{\partial x}, \frac{\partial f}{\partial z} = \frac{\partial h}{\partial x}, \frac{\partial g}{\partial z} = \frac{\partial h}{\partial y}. \quad (13)$$

Therefore, the potential generated by this segment in space (X, Y, Z) can be found by equation (15).

$$\phi_i = \int_{(x_{si}, y_{si}, z_{si})}^{(x_{ei}, y_{ei}, z_{ei})} -\frac{q}{4\pi rL} ds + C, \quad (14)$$

$$\phi_i = -\frac{q}{4\pi L}\left(\int_{x_{si}}^{x_{ei}} f(x, y_{si}, z_{si})dx + \int_{y_{si}}^{y_{ei}} g(x, y, z_{si})dy + \int_{z_{si}}^{z_{ei}} h(x, y, z)dz\right) + C, \quad (15)$$

which is

$$\phi_i = \int_{x_{si}}^{x_{ei}} -\frac{q}{4\pi rL}\frac{1}{s}(x - x_{si})dx + \int_{y_{si}}^{y_{ei}} -\frac{q}{4\pi rL}\frac{1}{s}(y - y_{si})dy + \int_{z_{si}}^{z_{ei}} -\frac{q}{4\pi rL}\frac{1}{s}(z - z_{si})dz + C. \quad (16)$$

In the three items on the right side of the equation, the first item x is the integral variable; then, the other two quantities y and z are constant, and the other two points are similar.

The integration is performed by the first item on the right:

$$\int_{x_{si}}^{x_{ei}} -\frac{q}{4\pi rL}\frac{1}{s}(x - x_{si})dx = -\frac{q}{4\pi L}\int_{x_{si}}^{x_{ei}} \frac{1}{r}\frac{1}{s}(x - x_{si})dx = -\frac{q}{4\pi L}\int_{x_{si}}^{x_{ei}} \frac{1}{\sqrt{(x - X)^2 + (y - Y)^2 + (z - Z)^2}} \cdot \frac{1}{\sqrt{(x - x_{si})^2 + (y - y_{si})^2 + (z - z_{si})^2}}(x - x_{si})dx. \quad (17)$$

Simplified equation, take $a = (y - Y)^2 + (z - Z)^2$, $b = (y - y_{si})^2 + (z - z_{si})^2$, then

$$= -\frac{q}{4\pi L}\int_{x_{si}}^{x_{ei}} \frac{1}{\sqrt{(x - X)^2 + a}} \frac{1}{\sqrt{(x - x_{si})^2 + b}}(x - x_{si})dx. \quad (18)$$

The function $f(x, y_{si}, z_{si}) = (1/\sqrt{(x - X)^2 + a})(1/\sqrt{(x - x_{si})^2 + b})(x - x_{si})$; then, equation (17) is equivalent to the function $f(x, y_{si}, z_{si})$, and the integral on the interval $[x_{si}, x_{ei}]$ is obtained.

Then, the potential generated by the entire horizontal well in space (X, Y, Z) is

$$\phi = \sum_{i=1}^{m} \phi_i = -\frac{q}{4\pi L}\sum_{i=1}^{m}\left(\int_{x_{si}}^{x_{ei}} f(x, y_{si}, z_{si})dx + \int_{y_{si}}^{y_{ei}} g(x, y, z_{si})dy + \int_{z_{si}}^{z_{ei}} h(x, y, z)dz\right). \quad (19)$$

Due to the positional relationship, there is a difference between the fluid confluence mode at both ends of the horizontal well in the oil layer and the fluid confluence mode in the middle part, and there is interference between the microelements of the wellbore, and a pressure drop in the fluid

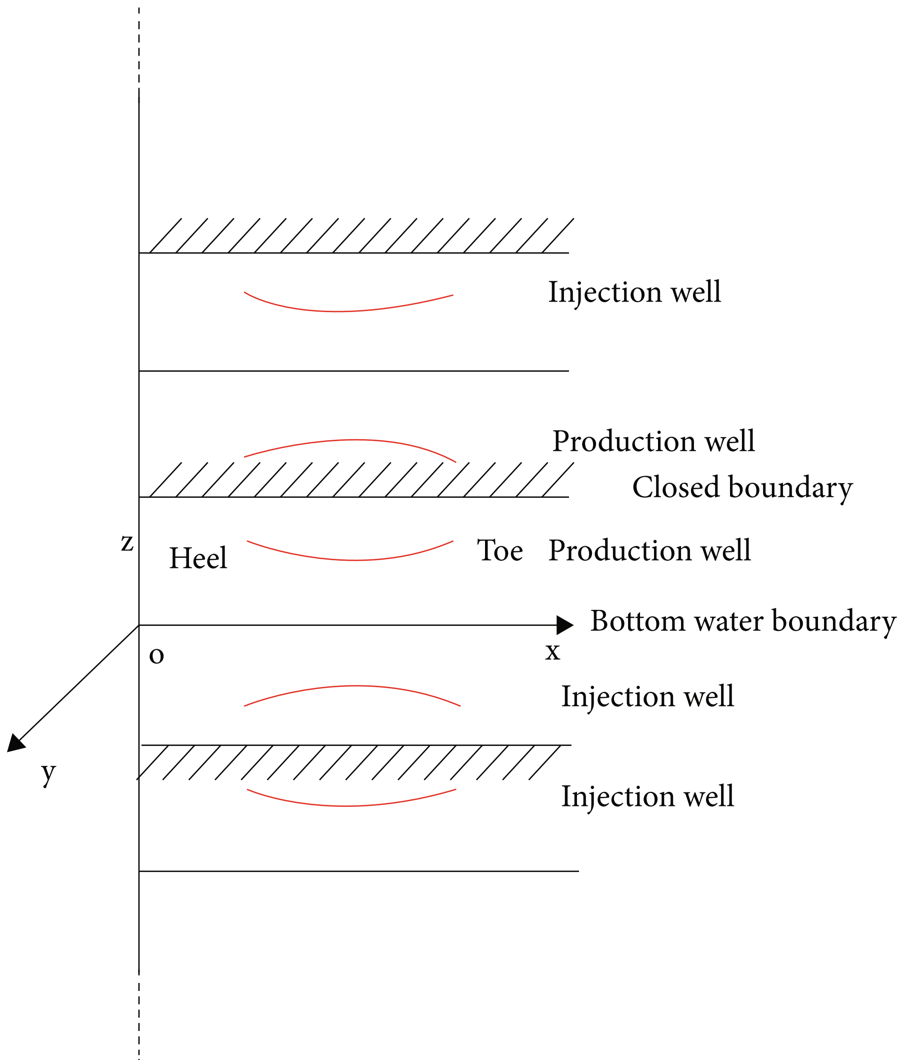

FIGURE 3: Mirror image of horizontal well in bottom water drive reservoir.

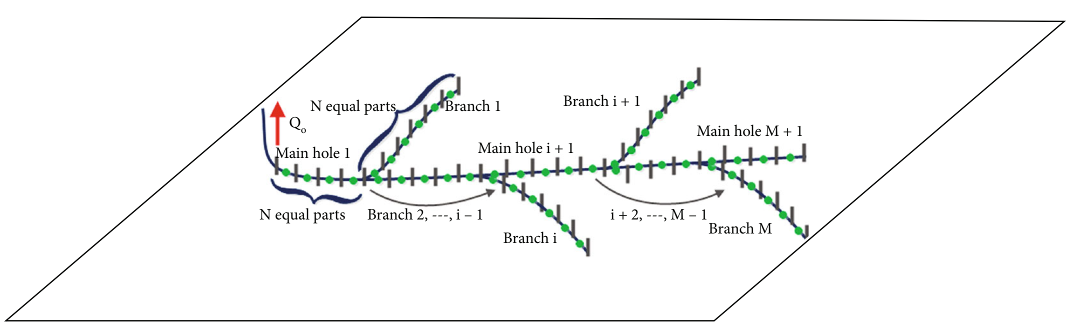

FIGURE 4: Microelement division of fishbone wells.

flow in the wellbore. The flow rate from the oil layer to the various parts of the horizontal wellbore is different. For this reason, a horizontal well is divided into a number of sections and lines. Since the length of each section of the line is very short, it is assumed that the fluid flows uniformly from the reservoir along the line, and the potential generated by each line is equivalent to the equation (19) of a horizontal well.

Oil well productivity predictions are also closely related to reservoir types. Generally, reservoir types can be distributed in four types: top closed bottom water reservoirs, gas top bottom water reservoirs, upper and lower closed edge water reservoirs, and upper and lower closed boundary reservoirs. Take top closed bottom water reservoirs as example. The calculation method of its potential is described below.

2.2. Calculation of Horizontal Well Potential in Top Closed Bottom Water Reservoir. For the top closed bottom water flooding reservoir shown in Figure 2, the horizontal well of length L is divided into N sections. According to the principle of mirror reflection, as shown in Figure 3:

$$\begin{aligned}\phi_j(X,Y,Z) = -\frac{q_j}{4\pi}\Bigg\{\sum_{n=-\infty}^{\infty}\big[&\xi_j(x,y,4nh+z,X,Y,Z)\\&+\xi_j(x,y,4nh+2h-z,X,Y,Z)\\&-\xi_j(x,y,4nh-z,X,Y,Z)\\&-\xi_j(x,y,4nh-2h+z,X,Y,Z)\big]\Bigg\}+C_j.\end{aligned} \quad (20)$$

In the equation, φ_j is the potential generated at any point in the reservoir by the line of segment j; q_j is the flow rate of the line of segment j; h is the oil-bearing thickness; z is the distance from each part of the well to the bottom of the reservoir; C_j is the constant; ξ is the function defined by the equation:

$$\begin{aligned}\xi_j(x,y,4nh+z,X,Y,Z) = \frac{1}{L_j}\sum_{i=1}^{m}\Bigg(&\int_{x_{si}}^{x_{ei}} f(x)dx+\int_{y_{si}}^{y_{ei}} g(y)dy\\&+\int_{4nh+z_{si}}^{4nh+z_{ei}} h(z)dz\Bigg),\end{aligned} \quad (21)$$

where L_j is the length of the j-th segment line; x_{s1} and x_{em} are the starting and ending abscissas in the x-axis direction of the j-th segment line, and the other parameters are the y and z direction coordinates.

2.3. Horizontal Well Flow Relationship. According to the principle of potential superposition, the potential of the entire horizontal well in the oil layer is

$$\phi(X,Y,Z) = \sum_{j=1}^{N}\phi_j(X,Y,Z)+C = -\sum_{j=1}^{N}\frac{q_j}{4\pi}\varphi_j+C. \quad (22)$$

For different types of reservoirs, φ_j in the equation is, respectively, equal to the expressions in curly brackets in equation (20). It can be obtained from equation (22)

$$\phi_e = \sum_{j=1}^{N}\phi_{je}+C, \quad (23)$$

which ϕ_e is the total potential function at the constant pressure boundary or the drain boundary; ϕ_{je} is the potential generated by the j-th segment line at the constant pressure boundary or the drain boundary.

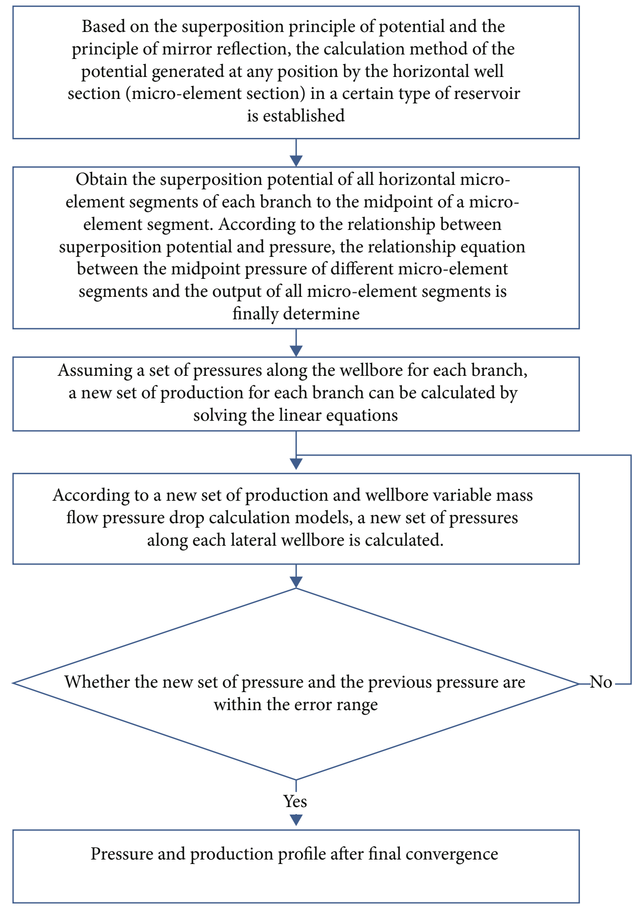

Figure 5: Flowchart of productivity calculation of fishbone well.

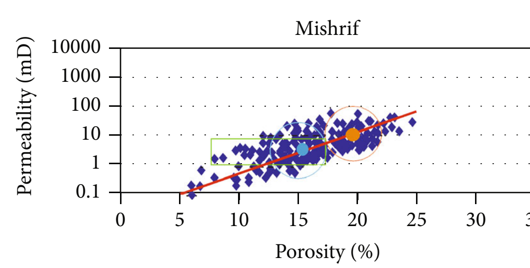

Figure 6: The relationship between porosity and permeability in Mishrif reservoir.

From equations (22) and (23), it can be obtained

$$\phi(X,Y,Z) = \phi_e + \sum_{j=1}^{N}\left[\phi_j(X,Y,Z)-\phi_{je}\right]. \quad (24)$$

According to the potential function

$$p(X,Y,Z) = \frac{\mu}{k}\phi(X,Y,Z)-\rho gh, \quad (25)$$

which p is the pressure at any point in the oil layer; k is the permeability of the oil layer; μ is the viscosity; ρ is the density; g is the acceleration of gravity.

Table 1: Formation test results of oilfield.

Well no.	Test horizon	Test well section m	Thickness m	Differential pressure MPa	Flow rate (oil) m^3/d	Test time hr	Oil production index $m^3/d/MPa$	Production index per-meter $m^3/(d\blacksquare MPa\cdot m)$
A	Mishrif	3873.8-3878.7	4.9	12.9	362.5	5	28.109	1.752
				8.16	770.7	34	94.427	5.903
B	Mishrif	3824.7-3829.9	14.6	6.38	1548.7	6.5	420.691	8.832
		3830.2-3839.7		4.27	1793.5	10		
				1.52	615.5	7.5		
				2.7	1102.1	3		
C	Mishrif	3840.9-3852.8	11.9	5.49	902.3	12	164.412	4.174
D	Mishrif	3972.9-3979.9	7	19	130.5	4	6.872	0.184
E	Mishrif	3957.9-3963.7	6.1	8.65	253.8	0.5	29.262	0.738
F	Mishrif	3824.7-3834.8	10.1	1.17	174.1	—	149.815	4.566

Table 2: Basic parameters of one fishbone well.

Geometric average permeability/mD	4	Length of main wellbore/m	600
Borehole diameter/mm	152.4	Reservoir thickness/m	72
Reservoir type	Top-sealed bottom water reservoir	Crude density/API	22.5
Crude viscosity/mPa.s	0.96	Production differential pressure/MPa	4
Crude volume factor	1.41	Saturation pressure/MPa	18.34

Table 3: Well completion and fluid property parameters of two horizontal wells.

Oilfield	Well name	Horizon	Reservoir thickness (average) m	Oil viscosity mPa.s	Oil volume factor	Horizontal wellbore length m	Wellbore diameter (inner) in	Geometric average permeability (horizontal and vertical) mD
A	A1	Mishrif MB21	**72**	0.96	1.4	198.24 (screen) + 442.76 (open hole)	5.8	**4.0**
	A2	Mishrif MB21	**72**	0.96	1.4	530.2 (open hole)	5.8	**4.0**
B	B1	Mishrif MB21	**35**	0.96	1.4	600.0	5.8	**4.0**
	B2	Mishrif MB21	**35**	0.96	1.4	600.0 (Assumed)	5.8	**4.0**

Substituting equation (24) into equation (25), it can be obtained

$$p(X, Y, Z) = p_e + \frac{\mu}{k}\sum_{j=1}^{N}\left[\phi_j(X, Y, Z) - \phi_{je}\right] - \rho g(Z - z_e), \tag{26}$$

where p_e and z_e are the pressures and Z coordinate at the corresponding boundaries, respectively.

2.4. Semianalytical Method for Describing Single-Phase Steady-State Variable Mass Flow in Fishbone Multilateral Wells. As shown in Figure 4, to simplify the description, it is assumed that the flow of each branch of the fishbone well corresponds to the first type of wellbore flow in a horizontal well, and the fishbone well is established to consider the mutual interference between the branches and the wellbore joints. In the coupled model, the pressure and the flow meet the momentum conservation, energy conservation, and mass conservation criteria at the junction of the branch and the main wellbores.

Assuming that there are M branches with branch lengths of L_i, the main wellbore is divided into $M + 1$ segments by the branches, and the lengths of the main wellbore segments are L_i ($i = M + 1, M + 2, \ldots, 2M$). Each section of the main wellbore and each branch is divided into N equal parts, that is, N microelement segments, to study not only the interaction among the internal microelement segments of each branch (main wellbore) but also the interaction among different branches (including the main wellbore). There is also an interaction among microelement segments. A total of 2

Table 4: Two-well production test data and prediction model error analysis.

Date	Well name	Choke size	Upstream pres.	Flow quantity				GOR	GLR	Water cut	Static pressure	Flow pressure (calculated by Pipesim)	$\triangle P$	Liquid production index (calculated)	Liquid production rate prediction	Absolute relative error
				Liquid	Oil	Water	Gas									
		∗/64	kg/cm^2	bbl/d	bbl/d	bbl/d	MMscf	scf/stb	scf/stb	%	MPa	MPa	MPa	bbl/d/psi	bbl/d	%
2018/6/26	A2	48	48	3088	3032	56	1.8082	596	586	1.8	32.7	28.6	4.17	5.1	2983.7	3.4
2018/1/3	A1	60	22.0	2965	2965.0	0.0	1.3019	439	439	0.0	26.8	22.3	4.45	4.6	2807.2	5.3
	B1	42.0	27.0	1702	1702	0.0				0.0	30.0	26.6	3.42	3.4	1471.2	13.6
	B2	54.0	21.0	1464	1464	0.0				0.0	27.9	24.7	3.19	3.2	1360.5	7.1
Average																7.3

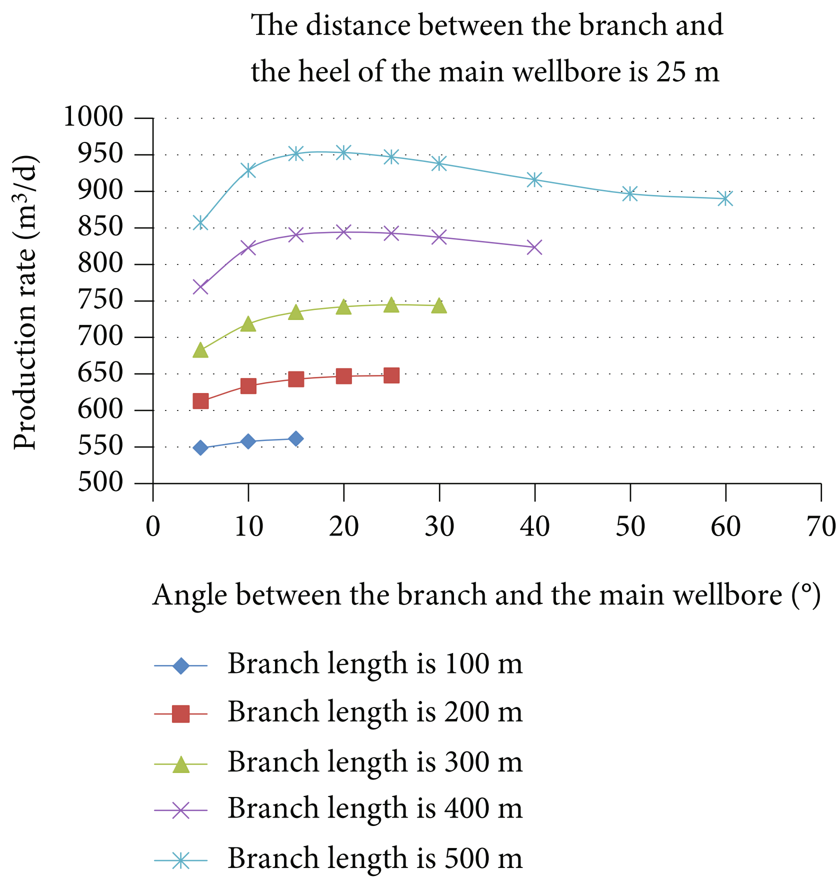

(a) Lateral well position is 25 m from the heel of the main wellbore

Figure 7: Continued.

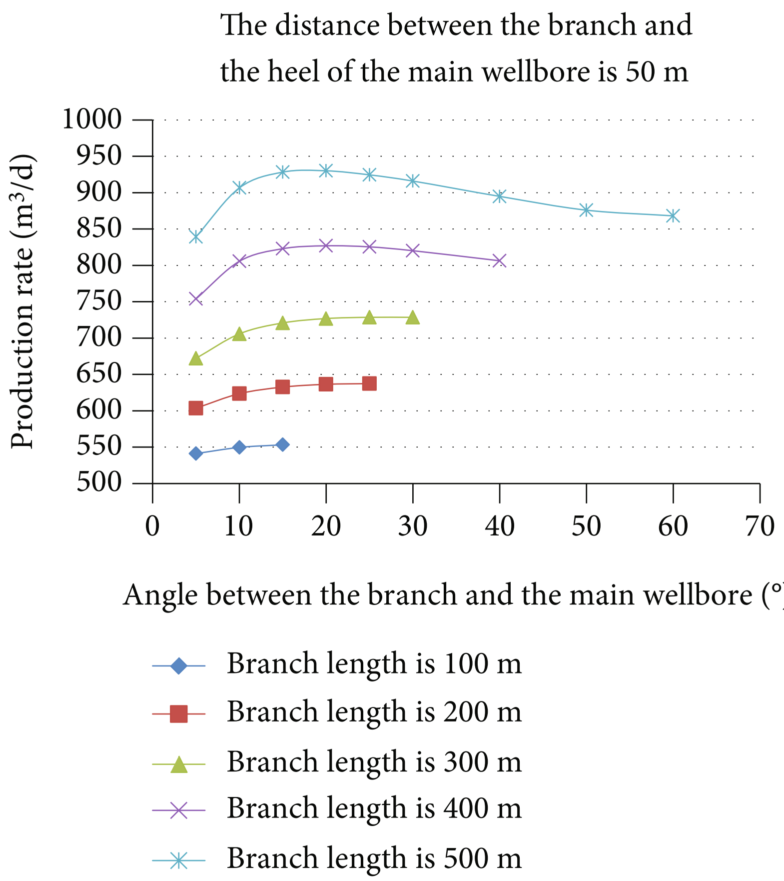

(b) Lateral well position is 50 m from the heel of main wellbore

Figure 7: Continued.

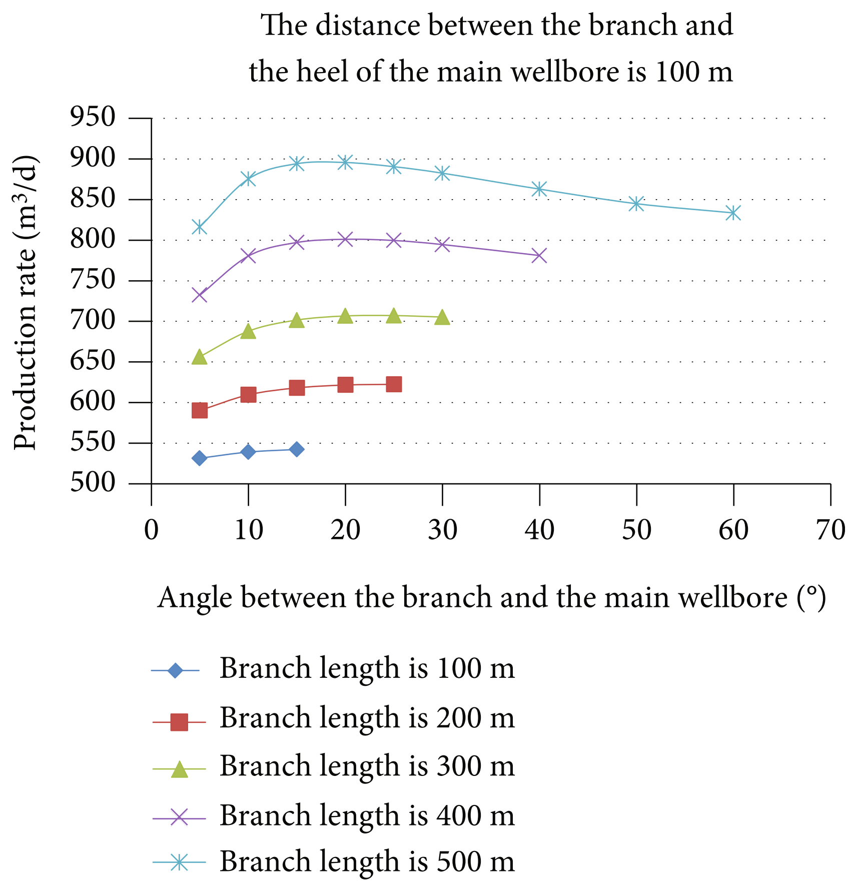

(c) Lateral well position is 100 m from the heel of the main wellbore

Figure 7: Continued.

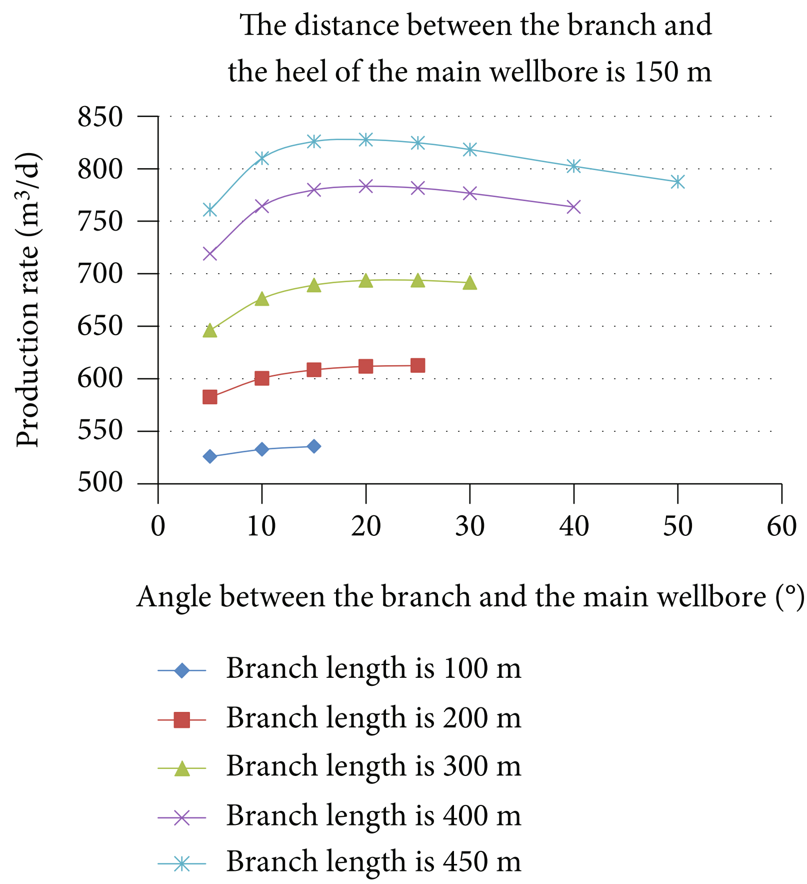

(d) Lateral well position is 150 m from the heel of the main wellbore

Figure 7: Production with different angles between the lateral well and main wellbore.

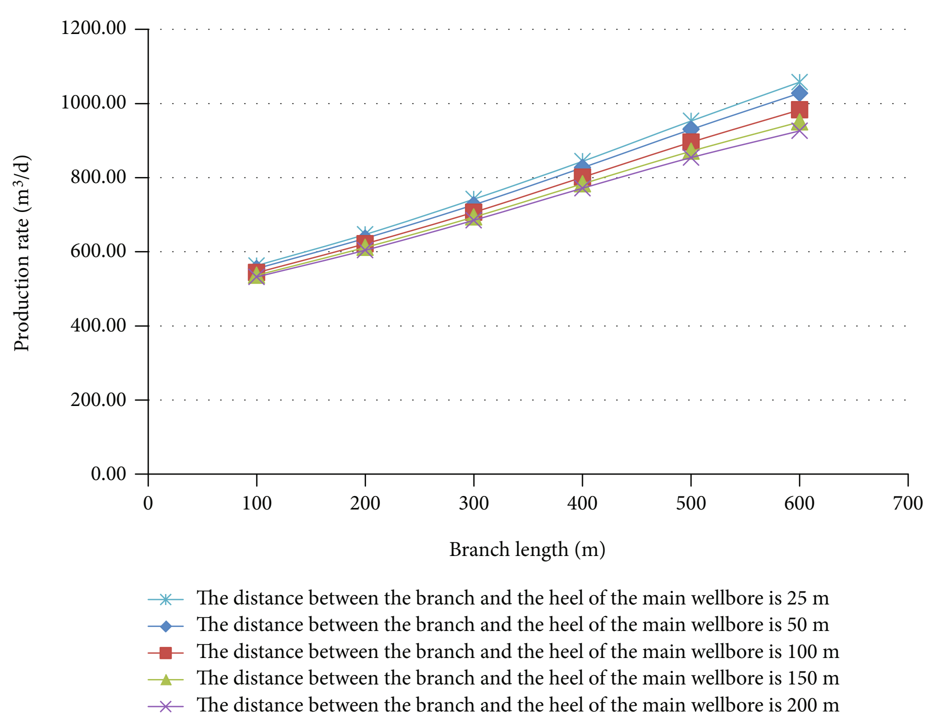

Figure 8: Production with different branch lengths.

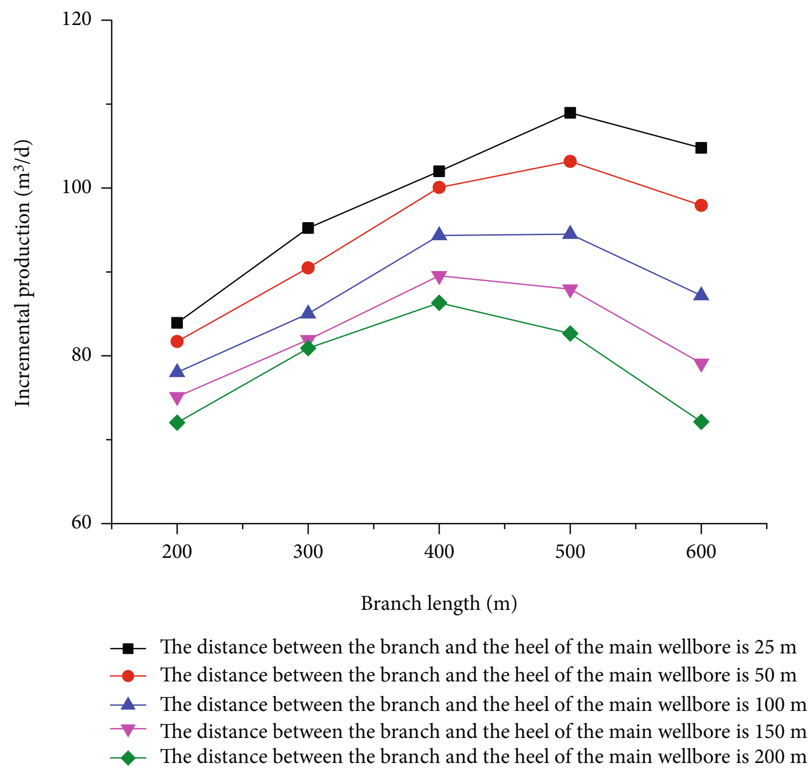

Figure 9: Incremental production with different branch lengths.

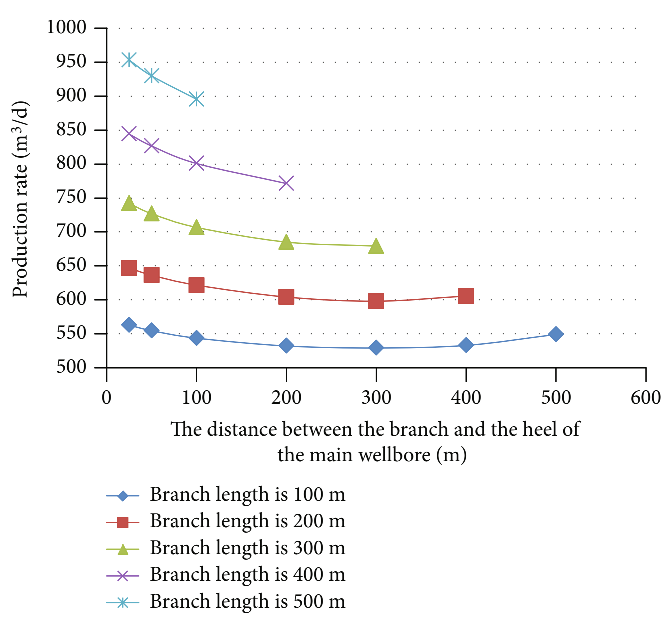

Figure 10: Production rates with different branch positions.

$M+1$ segments, M branch and $M+1$ main wellbores segments, are labeled in order, with the main wellbore segments last. Let the pressure at the midpoint of the m segment of the n branch be $p_{w,n,m}$, and set the potential of the j segment of the i branch at the midpoint of the m segment of the n branch to $\Phi_{i,j,n,m}$; according to equation (26), obtain

$$p_{w,n,m} = p_e + \frac{\mu}{k}\sum_{i=1}^{2M+1}\sum_{j=1}^{N}\left(\phi_{i,j,n,m} - \phi_{i,j,e,e}\right) + \rho g\left(z_e - z_w\right)\left(n = 1, 2, \cdots, 2M+1;\, m = 1, 2, \cdots, N\right). \quad (27)$$

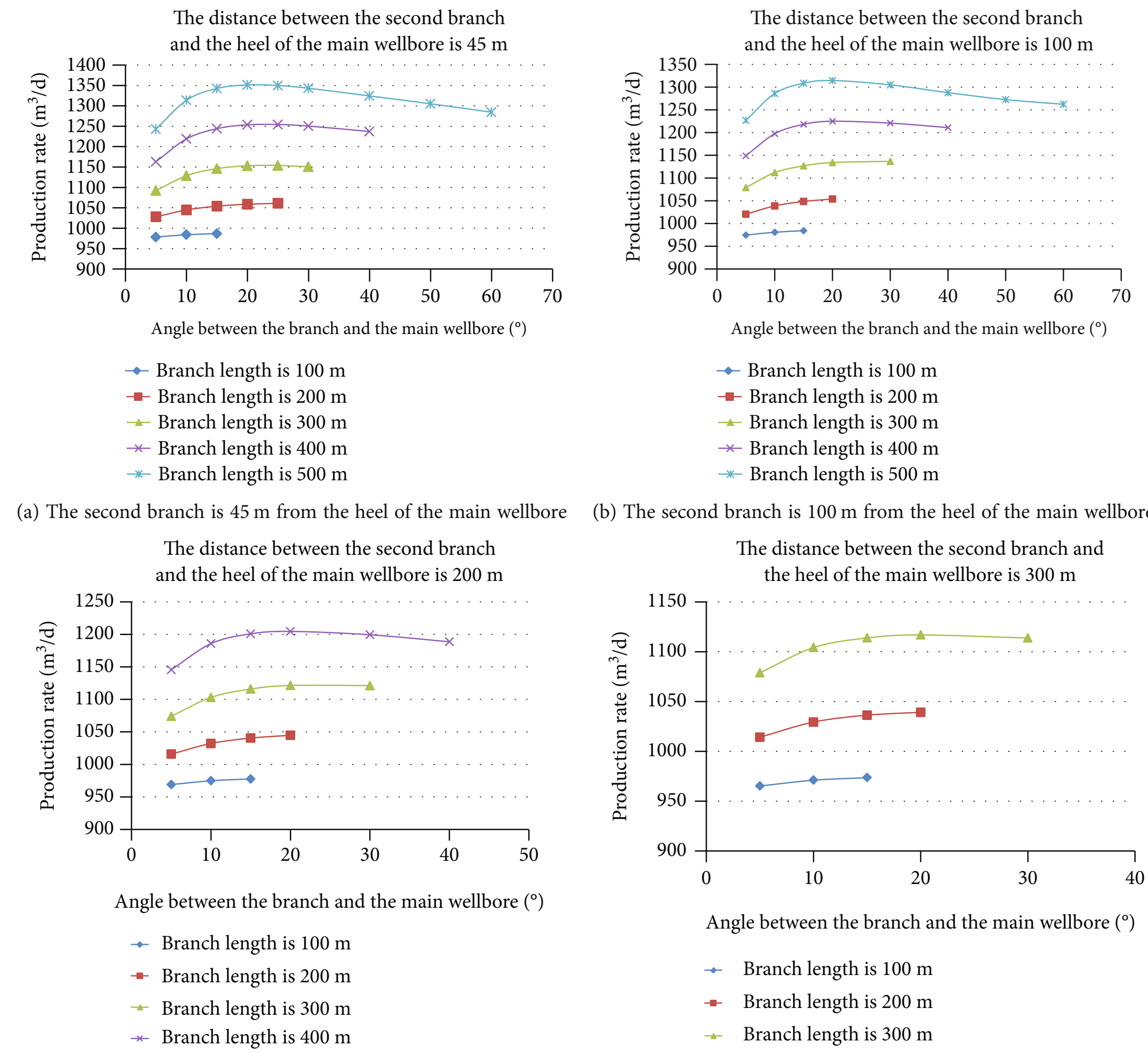

(a) The second branch is 45 m from the heel of the main wellbore (b) The second branch is 100 m from the heel of the main wellbore

(c) The second branch is 200 m from the heel of the main wellbore (d) The second branch is 300 m from the heel of the main wellbore

FIGURE 11: Production rates with different angles between the second branch and main wellbore.

The upper form is deformed.

$$\sum_{i=1}^{2M+1}\sum_{j=1}^{N}\lambda q_{i,j}\left(\phi_{i,j,n,m}-\phi_{i,j,e,e}\right)=p_e-p_{w,n,m}+\rho g\left(z_e-z_w\right), \tag{28}$$

where $\lambda=\mu/4\pi k$.

The pressure at the midpoint of segment j in branch i is

$$p_{w,i,j}=p_{1,i,j}-0.5dp_{w,i,j}(i=1,2,\cdots,2M+1\,;j=1,2,\cdots,N), \tag{29}$$

where $p_{2,i,N}=p_{wf}$ and p_{wf} are the flow pressures at the wellbore heel.

$$p_{1,i,1}=p_{2,i+1,N}=p_{2,i-M,N}(i=M+1,M+2,\cdots,2M), \tag{30}$$

$$p_{2,i,j}=p_{1,i,j}-\Delta p_{w,i,j}(i=1,2,\cdots,2M+1\,;j=1,2,\cdots,N), \tag{31}$$

$$p_{1,i,j+1}=p_{2,i,j}(i=1,2,\cdots,2M+1\,;j=1,2,\cdots,N-1). \tag{32}$$

Total well production is

$$Q_o=\frac{\sum_{i=1}^{2M+1}\sum_{j=1}^{N}q_{s,i,j}}{B_o}. \tag{33}$$

In the above coupling model, q and p_w are both unknowns and can be solved by an iterative method. First, assume a set of p_w values, solve for q with equation (28), then substitute q into the pressure drop formula and equation (29) to update p_w from the heel to the toe or branch of the main wellbore, and then by equation (28) to update q, and repeat until q and p_w both reach a certain calculation

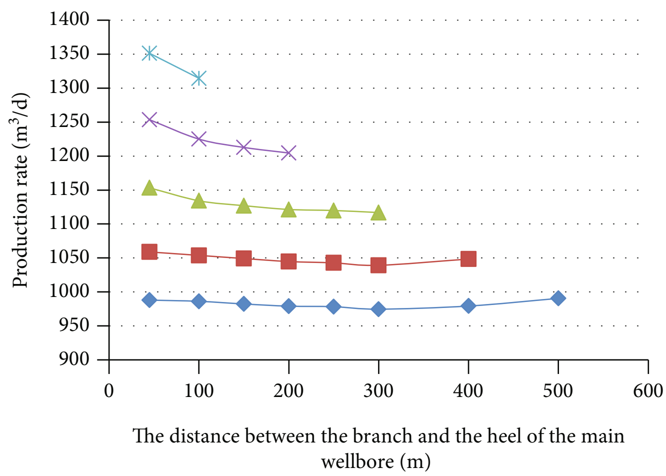

Figure 12: Production rates with different positions of the second branch.

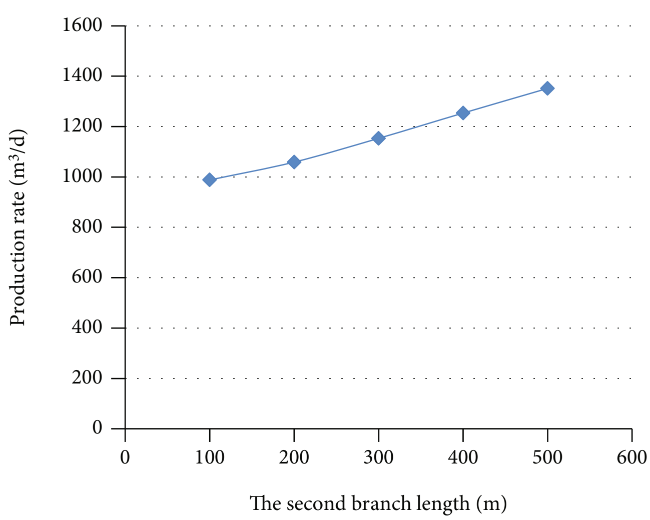

Figure 13: Production with different length conditions of the second branch.

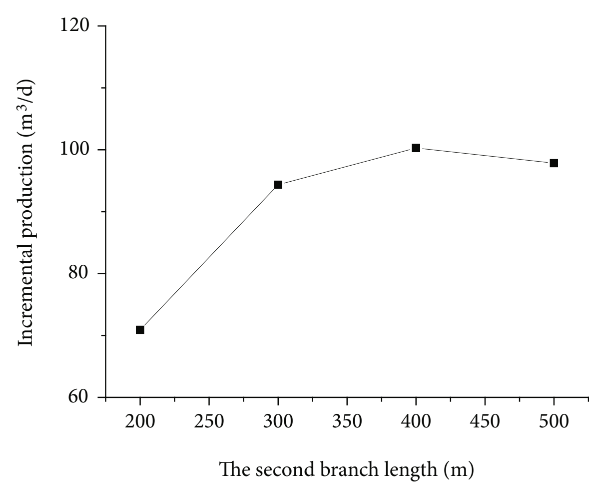

Figure 14: Incremental production with different length conditions of the second branch.

accuracy. Finally, the well production of the whole well is obtained from equation (33).

2.5. Calculation Flowchart. The flowchart is shown in Figure 5 below.

3. Capacity Prediction and Parameter Sensitivity Analysis of One Lateral Branch of a Fishbone Well

The target oil reservoir is the Msihrif reservoir. According to the statistical data of the sequence stratigraphic map of logging interpretation, different oil layers in the Mishrif reservoir are divided into two grades: good oil layer and poor oil layer. According to the porosity-permeability relationship data of the target oilfield Msihrif (Figure 6) and the formation test data of oilfield (Table 1), it can be seen that, except for a small part of the low permeability reservoirs, the meter oil recovery index is relatively small. The rest can also be divided into two grades, corresponding to the oil layers.

As can be seen from Figure 6, the average permeability of the two grades is about 4 mD and 10 mD, respectively.

The basic parameters of a reservoir in the target Oilfield are shown in Table 2. Taking the three horizontal well parameters and measured data of the target oilfield as an example (the parameters are shown in the following two Tables 3 and 4), capacity prediction is carried out with the established model. The calculation results show that the

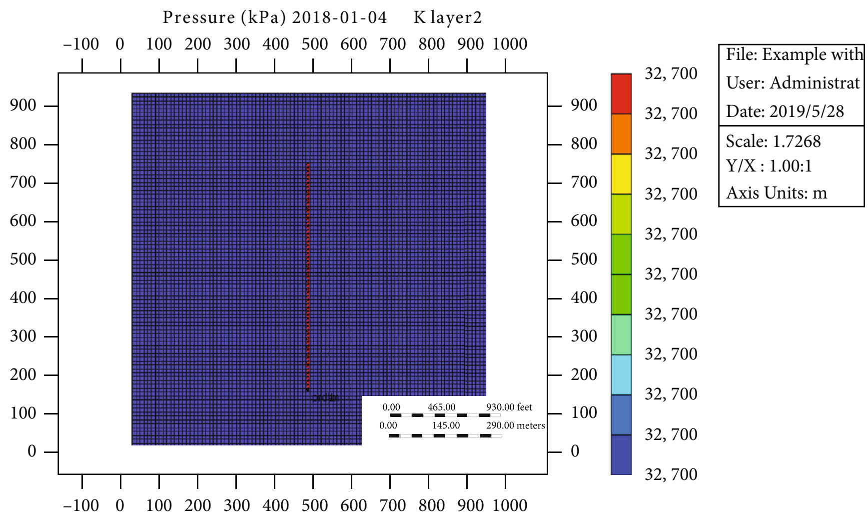

Figure 15: Establishment of the CMG digital analog model.

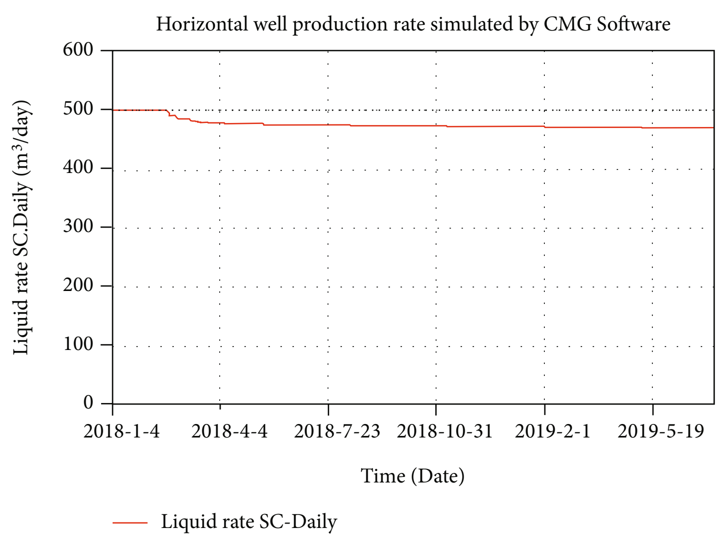

Figure 16: CMG simulation results.

model calculation error is small. The average error is within the acceptable range of engineering calculations.

According to the investigation, the factors affecting the productivity of fishbone multilateral wells can be divided into two categories: lateral distribution parameters (symmetry of branches, the same and different sides of branches, and the location of branches points) and lateral shape parameters (branch angle, number of branches, branch length, and branch spacing)[15–17].

3.1. Analysis of the Influence of the Angle between a Branch and the Main Wellbore on the Production Capacity. Under the same reservoir properties, fluid properties, and other conditions, calculate the production of lateral wells with different angles between the branch and the main well, see Figure 7 for the results. The figure shows that the production is greatest when the angle between the branch and the main wellbore is 15~20°.

3.2. Analysis of the Influence of Branch Length on Production Capacity. Under the same reservoir properties, fluid properties, and other conditions, calculate the production of fishbone multilateral wells with different lengths of branch, see Figures 8 and 9 for the results. Figure 9 shows that the production is higher when the length of a branched well is 500 m.

3.3. Analysis of the Impact of Branch Location on Production Capacity. Under the same reservoir properties, fluid properties, and other conditions, calculate the production of branched wells with different location conditions, see Figure 10 for the results. This figure shows that it is

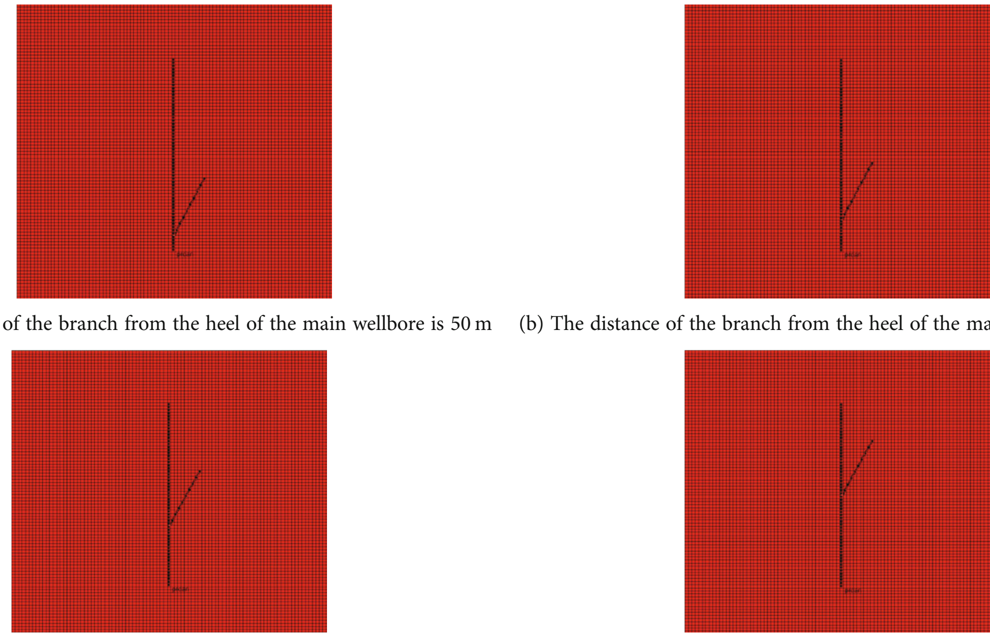

(a) The distance of the branch from the heel of the main wellbore is 50 m (b) The distance of the branch from the heel of the main wellbore is 100 m

(c) The distance of the branch from the heel of the main wellbore is 200 m (d) The distance of the branch from the heel of the main wellbore is 300 m

FIGURE 17: CMG model establishment with different branch positions.

recommended that the branched well is started 25 m from the heel of the main wellbore.

4. Productivity Prediction and Parameter Sensitivity Analysis of Two Lateral Branches of a Fishbone Well

4.1. Analysis of the Influence of the Angles between the Branches and the Main Wellbore on the Productivity. When the first branch is positioned 25 m from the heel of the main wellbore and 500 m in length, and the angle between the branch and the main wellbore is 20° (the optimal result of the first branch), under the condition that the reservoir properties, fluid properties, and other conditions remain unchanged, the production rates of the two branched wells at different angles to the main wellbore are calculated, see Figure 11 for the results. This figure shows that the most favorable angle between the second branch and the main wellbore is 15~20°.

4.2. Analysis of the Impact of Branch Location on Production Capacity. When the distance between the first branch and the heel of the main wellbore is 25 m, the length is 500 m, and the angle between the branches and the main wellbore is 20° (the optimization result of one fishbone well), under the condition that the reservoir properties, fluid properties, and other conditions remain unchanged, the production rates of the two branched wells in different positions are calculated, see Figure 12 for the results. This figure shows that the second branch positioned 45 m from the heel of the main wellbore is most favorable for production.

4.3. Analysis of the Influence of the Second Branch Length on Production Capacity. When the distance between the first branch and the heel of the main wellbore is 25 m, the length is 500 m, and the angle between the branches and the main well is 20° (the optimal result of one branched well), under the condition that the reservoir properties, fluid properties, and other conditions remain unchanged, and the distance between the second branch and the heel of the main wellbore is 45 m, the production rates of the two branched wells with different length conditions are calculated, see Figures 13 and 14 for the results. These figures show that the most favorable length of the second branch is 500 m.

4.4. Sequence of Factors That Affect Production Capacity. It can be seen from the simulation of single and double branches lateral wells that, within the respective ranges of different influencing factors, the factors affecting the productivity of lateral wells from large to small are branch length or main wellbore length, branch position, and branch angle.

5. Numerical Simulation Verification of the Development of One Fishbone Well

The basic parameters of the horizontal wells are shown in Table 2. The self-built model and simulation software from the Computer Modeling Group, Ltd. (CMG; Alberta, Canada) (see Figure 15) are used to predict production. CMG is a three-phase black oil simulation software that considers gravity and capillary force. The network system can use rectangular coordinates, radial coordinates, and variable depth/variable thickness coordinates. In any network system, two- or three-dimensional models can be established. The model selected in the CMG software is the Implicit-explicit Black Oil Simulator (IMEX), which is an adaptive implicit black oil simulator (adaptive implicit numerical simulation method) for simulating the flow of water, oil-water, and

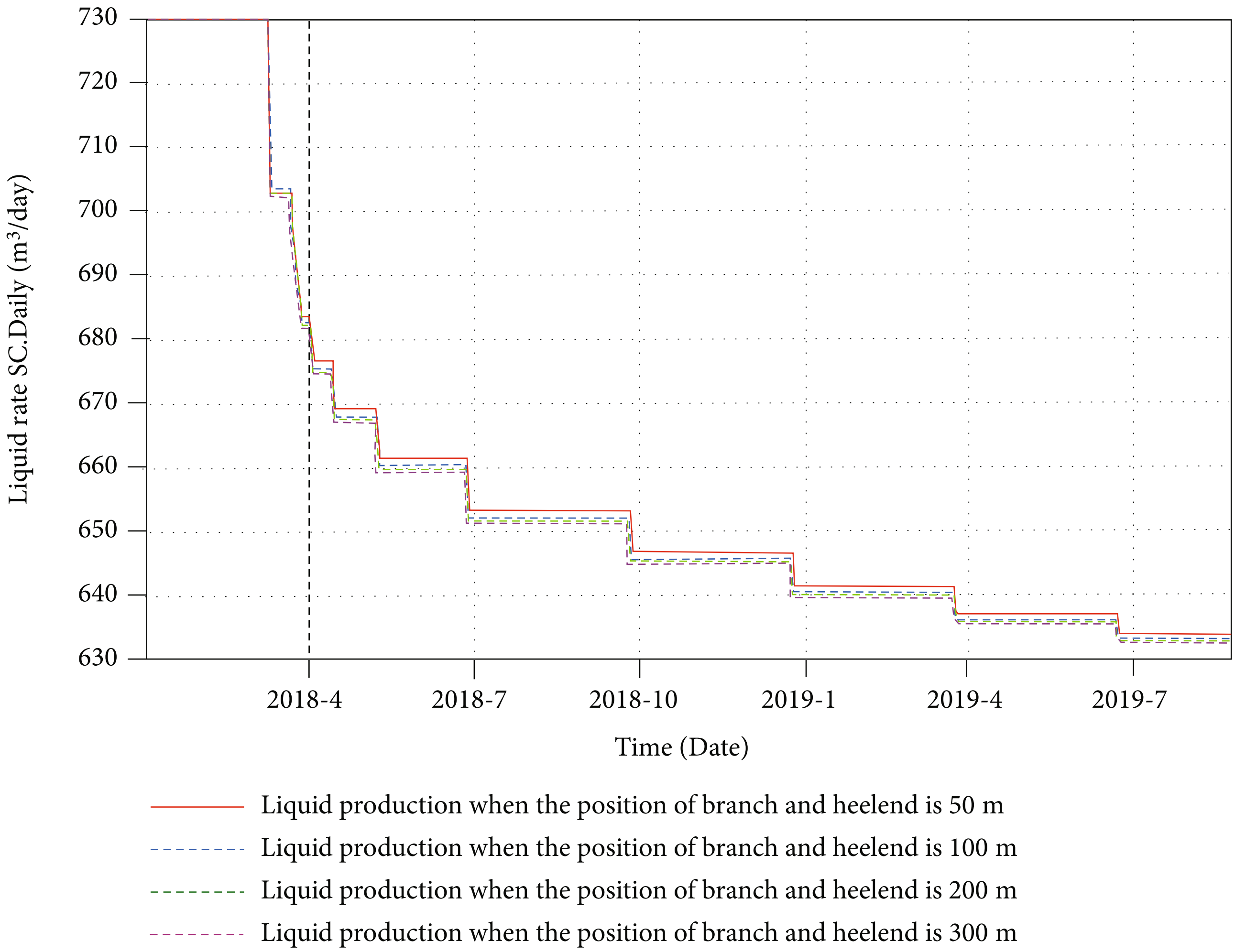

Figure 18: Production with different branch positions.

oil-gas-water reservoir fluids. IMEX can run in three modes: display, fully implicit, and adaptive implicit. In most cases, only a small part of the mesh needs to be solved fully implicitly, and most of the grids can be solved by explicit methods. The adaptive implicit method is the solution method suitable for this situation, and in thinly layered oil reservoirs, high-speed flow coning problems will occur during production. It is very effective to adopt adaptive implicit processing to address these problems. Using adaptive implicit options can reduce the computational run time by one-third to half. This calculation can use the same large time step as the fully implicit method. The user can specify the grid to be calculated by the fully implicit method, and the network that uses the fully implicit calculation can be dynamically selected according to the user-defined limit or matrix conversion critical value grid.

On the basis of the reservoir, fluid, and oil well parameters, simulation mechanism models for branched well flow are established using the CMG FlexWell function. The grid size is $92 \times 92 \times 4\,m^3$ (a high number of meshes with small computational error has been established), each horizontal grid is 10 m, and each vertical grid of the top three grids is 24 m. The formation grid is a constant pressure water layer (provided by a water injection well). The horizontal well or the main wellbore of the fishbone well is located in the middle level of the grid, and its length is 600 m.

The production of the self-built model is $488.06\,m^3/d$. The calculation results of the digital model are shown in Figure 16. By comparing the calculation results with historical oil well production data, it can be seen that the prediction results of the self-built model and digital model are consistent, which verifies the reliability of the self-built model.

5.1. Analysis of the Impact of Branch Location on Production Capacity. Assuming that the branch length is 200 m and that the angle between the branch and the main wellbore is 20° under the condition of constant reservoir properties and fluid properties, the production rates of the branched well with different branch positions are calculated (Figure 17). The results are shown in Figure 18. The figure shows that the farther the branch is from the heel of the main wellbore (not exceeding the length of the main well), the lower the

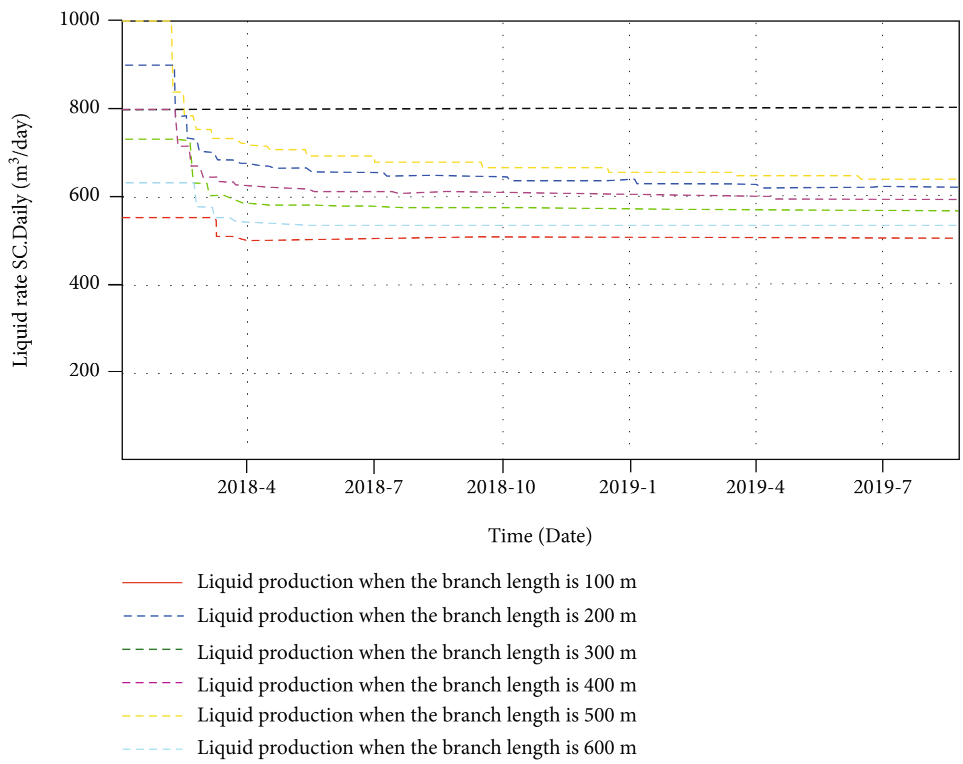

FIGURE 19: Production with different branch lengths.

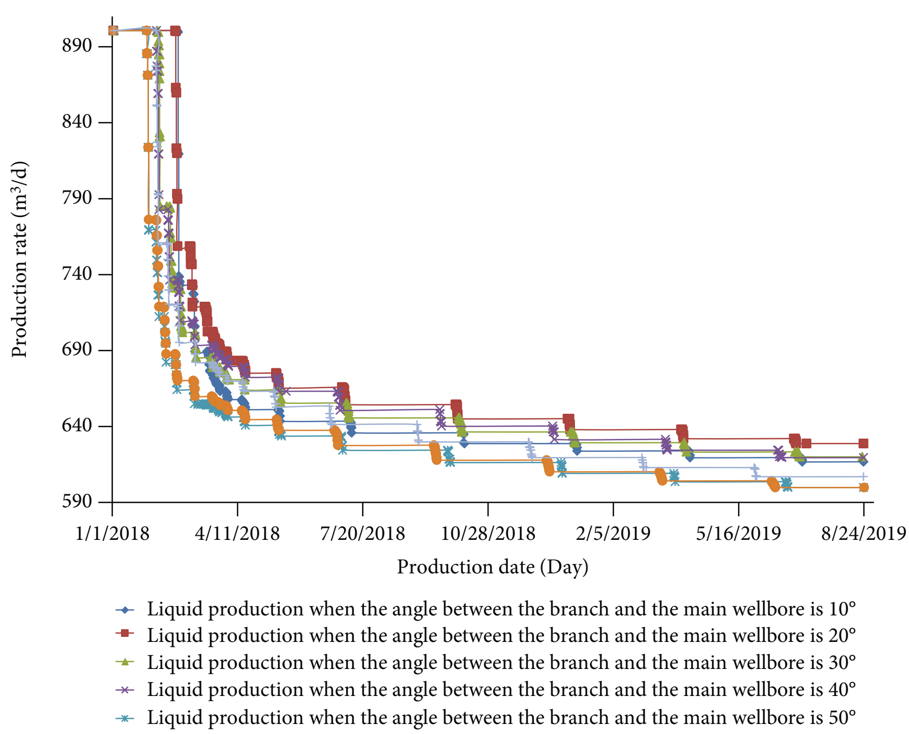

FIGURE 20: Production with different angles between the branch and main well (detailed).

production is, which is consistent with the prediction rule of the new model.

5.2. Analysis of the Influence of Branch Length on Production Capacity. Under the condition of the same reservoir property and fluid property, assuming that the heel of the main wellbore is 50 m from the branch and that the angle between the branch and the main wellbore is 20°, the production rates of branched wells with different branch lengths are calculated. Figure 19 shows that with increasing branch length, the production increases, but when the branch increases from 500 m to 600 m, the increase in production decreases. Therefore, the branch length of 500 m is most favorable, which is consistent with the prediction result of the new model.

5.3. Analysis of the Influence of the Angle between the Branch and the Main Wellbore on the Productivity. Assuming that the length of the branch is 500 m and the location of the branch from the heel of the main wellbore is 50 m, the production rates of the branched well are calculated with different angles between the branch and the main wellbore, and the results are shown in Figures 20. It can be seen from these figures that when the angle between the branch and the main wellbore is approximately 20°, the production is maximized, which is consistent with the result of the new model.

5.4. Sequence of Factors That Affect Production Capacity. It can be seen from the simulation of single and double branches lateral wells by CMG that, within the respective ranges of different influencing factors, the factors affecting the productivity of lateral wells from large to small are branch length or main wellbore length, branch angle, and branch position. This is the same as the prediction of the model established in this paper.

6. Conclusion

Aiming at productivity prediction and parameter optimization of branched wells in target oilfields, a coupling model of fishbone wells considering the mutual interference of formation seepage between branches and the interaction of wellbore connections is established and solved. The productivity prediction and parametersdesign optimization of fishbone wells are carried out after the verification of the self-built model and CMG model with field-measured data. The results are as follows.

(1) A single-branch fishbone well is used for model development. The recommended branch length is 500 m, the angle between the branch and the main wellbore is 15~20°, and the branch position along the main wellbore is 25 m from the heel of the main wellbore

(2) A two-branch fishbone well is used for further model development. It is recommended that the length of both branches is 500 m, the angle between the branches and the main wellbore is 15~20°, the position of the first branch is 25 m from the heel of the main wellbore, and the position of the second branch is 45 m from the heel of the main wellbore

(3) The proposed model and CMG model are used to analyze the sensitivity of the production results to different parameters of a fishbone well, and the results of the two methods are consistent, which proves that the new model is reliable

(4) Within the respective ranges of different influencing factors, the factors affecting the productivity of lateral wells from large to small by the prediction results of the model established in this paper are branch length or main wellbore length, branch angle, and branch position. This is same from the prediction of the CMG

Data Availability

No data were used to support this study.

Conflicts of Interest

The authors declare that they have no conflicts of interest to report regarding the present study.

Acknowledgments

Thanks are due to Hu Haixia for serving as the corresponding author for the article. This work was supported by the National Natural Science Fund Project (62173049), major national projects (2016ZX05056004-002), and the open fund project “Study on transient flow mechanism of fluid accumulation in shale gas wells” of the Sinopec Key Laboratory of Shale Oil/Gas Exploration and Production Technology.

References

[1] X. Wei and X. Wu, “Enhancing oil recovery using multilateral well,” in *International Symposium on "Enhanced Oil Recovery Technology for High Water cut Reservoir" of the 2006 Annual Meeting of the Steering Committee and Academic Committee of the Center for Enhanced Oil Recovery*, Research Center for improving oil and gas recovery of Sinopec, 2006.

[2] R. Basquet, J. P. Caltagirone, F. G. Alabert, and J. C. Batsalle, “A semianalytical approach for productivity evaluation of complex wells in multilayered reservoirs,” *Spe Reservoir Evaluation & Engineering*, vol. 2, no. 6, pp. 506–513, 1999.

[3] A. Retnanto, T. P. Frick, C. W. Brand, and M. J. Economides, “Optimal configurations of multiple-lateral horizontal wells,” in *Paper presented at the SPE Western Regional Meeting*, Anchorage, Alaska, 1996.

[4] H. Yao, C. Shiqing, H. Youwei, and Y. Haiyang, “Transient pressure analysis of fishbone multi-lateral horizontal well with non-uniform flux density,” *Journal of Shenzhen University Science and Engineering*, vol. 33, no. 2, pp. 202–210, 2016.

[5] L. Chunlan and Z. Shicheng, “Productivity equation of fishbone shaped wells in steady state,” *Journal of Daqing Petroleum Institute*, vol. 34, no. 1, pp. 56–59, 2010.

[6] L. Chunlan, C. LinSong, and S. Fuji, "Derivation of productivity formulae of a fishbone well," *Journal of Southwest Petroleum Institute*, vol. 6, pp. 36-37, 2005.

[7] L. X. Ping, Z. Z. Shun, C. G. U. I. Xiang, W. J. Lu, and Y. F. Xin, "Inflow performance relationship of a herringbone multilateral well," *Acta Petrolei Sinica*, vol. 21, no. 6, pp. 57–60, 2000.

[8] D. Yonggang, C. Wei, H. Tianhu, and Y. Xiaoyong, "Seepage characteristics and unsteady pressure performance of multilateral wells," *Journal of Xi'an Shiyou University*, vol. 22, no. 2, pp. 136–138, 2007.

[9] A. Yongsheng, L. Zhenquan, Z. Shiming, and D. Chongrui, "Study on optimization theory and method of herringbone well configuration," *Petroleum Geology and Recovery Efficiency*, vol. 18, no. 4, pp. 82–85, 2011.

[10] A. Yongsheng, "Analysis of influences of the reservoir anisotropy on productivity of herringbone multi-lateral well," *Journal of Southwest Petroleum University*, vol. 33, no. 3, pp. 145–148, 2011.

[11] D. Le Ping, C. X. Zhimin, M. Fei, and L. Wei, "A coupling model of fishbone multilateral horizontal well in bottom water reservoir," *Journal of Southwest Petroleum University*, vol. 37, no. 4, pp. 117–126, 2015.

[12] W. Luo, R. Liao, X. Wang, M. Yang, W. Qi, and Z. Liu, "Novel coupled model for productivity prediction in horizontal wells in consideration of true well trajectory," *Journal of Engineering Research*, vol. 6, no. 4, pp. 1–21, 2018.

[13] Q. Wang, J. Yang, and W. Luo, "Flow simulation of a horizontal well with two types of completions in the frame of a wellbore–annulus–reservoir model," *FDMP-Fluid Dynamics & Materials Processing*, vol. 17, no. 1, pp. 215–233, 2021.

[14] P. Liu, Q. Wang, Y. Luo, Z. He, and W. Luo, "Study on a new transient productivity model of horizontal well coupled with seepage and wellbore flow," *PRO*, vol. 9, no. 12, p. 2257, 2021.

[15] Z. Shiming, Z. Yingjie, and S. Yong, "Design optimization for the horizontal well pattern with herringbone-like laterals," *Petroleum Exploration and Development*, vol. 38, no. 5, pp. 606–612, 2011.

[16] J. Kai, L. Min, H. Zhixiong, and X. Guoqing, "Analysis for transient deliverability of herringbone gas well and optimum configuration of lateral holes," *Journal of Southwest Petroleum University*, vol. 35, no. 6, pp. 127–132, 2013.

[17] Z. Dianfeng, "Wellbore flow characteristics and its influencing factors of fish-bone branch horizontal wells," *Fault Block Oil and Gas Field*, vol. 19, no. 6, pp. 796–799, 2012.